Supplementary Material

Figure S1

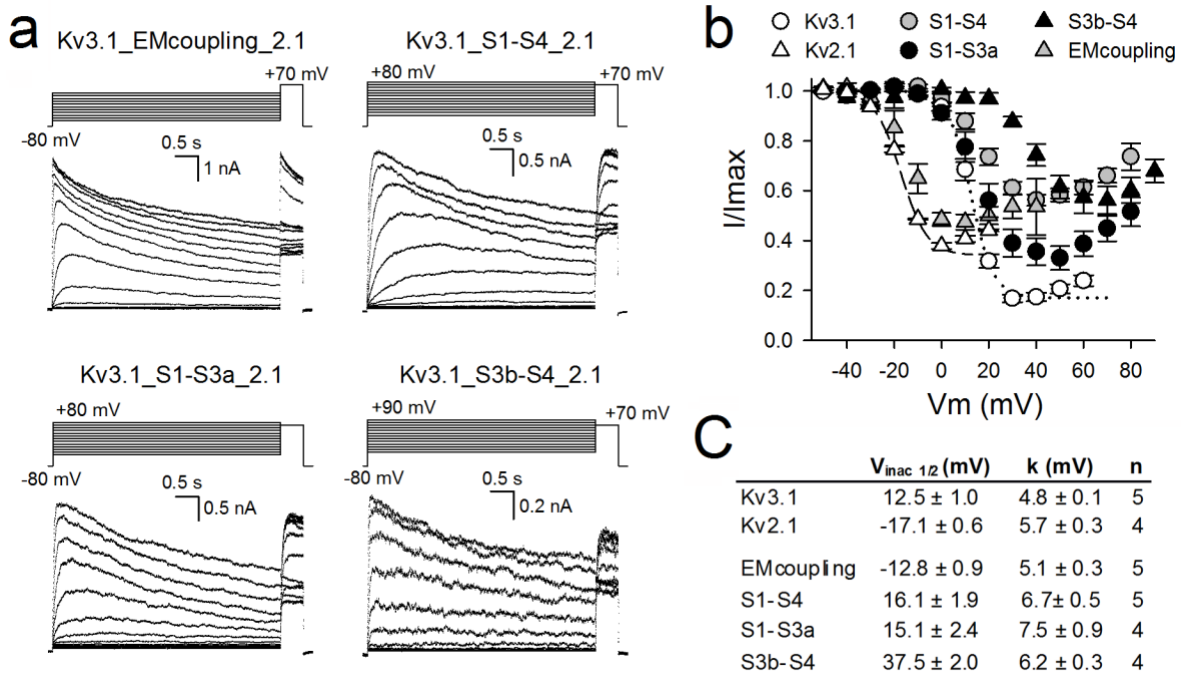

c

	$V_{inac\ 1/2}$ (mV)	k (mV)	n
Kv3.1	12.5 ± 1.0	4.8 ± 0.1	5
Kv2.1	-17.1 ± 0.6	5.7 ± 0.3	4
EMcoupling	-12.8 ± 0.9	5.1 ± 0.3	5
S1-S4	16.1 ± 1.9	6.7± 0.5	5
S1-S3a	15.1 ± 2.4	7.5 ± 0.9	4
S3b-S4	37.5 ± 2.0	6.2 ± 0.3	4

Figure S1. Voltage dependence of inactivation for the chimeric channels.

Panel **a** shows representative ionic current recordings to determine the inactivation process in the chimeras Kv3.1_EMcoupling_2.1, Kv3.1_S1-S4_2.1, Kv3.1_S1-S3a_2.1, and Kv3.1_S3b-S4_2.1 elicited by applying depolarization steps from a -80 mV holding potential (pulse protocols are shown on top and inter-pulse time was 20 s). Note the gradual decrease in current amplitude during the 5 s depolarization step. To estimate the degree of channel inactivation, a +70 mV test pulse was applied after the 5 s depolarization step. Panel **b** displays the voltage dependence of channel inactivation for WT Kv3.1 (white circles and with the dotted line representing the average Boltzmann fit), WT Kv2.1 (white triangles and dashed line), Kv3.1_EMcoupling_2.1 (gray triangles), Kv3.1_S1-S4_2.1 (gray circles), Kv3.1_S1-S3a_2.1 (black circles), and Kv3.1_S3b-S4_2.1 (black triangles). Data were obtained by plotting the normalized current during the +70 mV test pulse as a function of the pre-pulse depolarization potential. Note that all channels displayed a U-type inactivation profile and the amount of channel inactivation is less at stronger depolarizations. Panel **c** lists for the different channels the mean $V_{inac\ ½}$ and slope factor k value ± S.E.M. with n the number of cells analyzed. Parameters were obtained by approximating the voltage dependence of channel inactivation (plots in panel b) with a Boltzmann equation (see material and methods section).

Figure S2

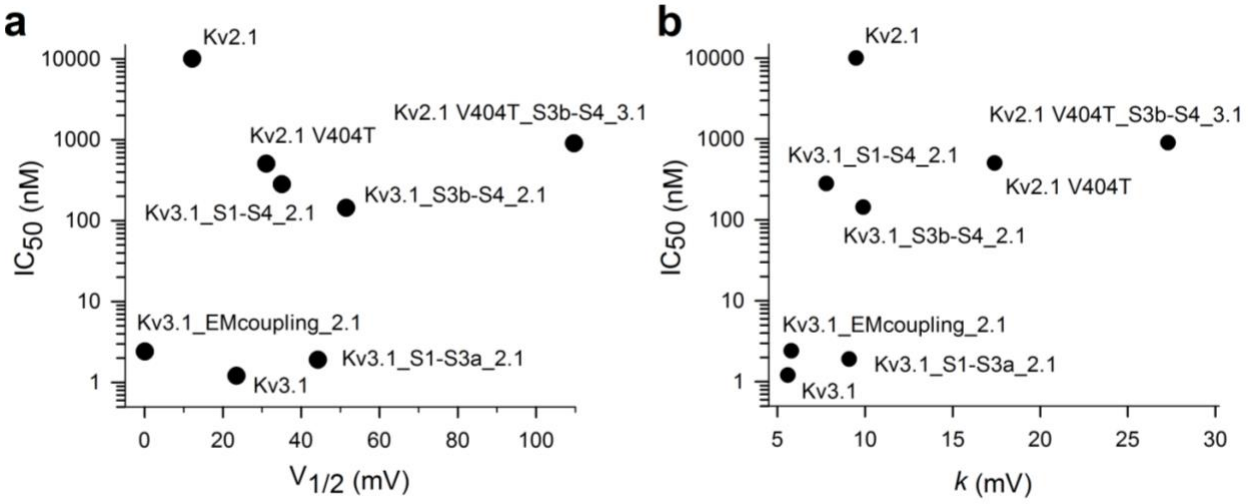

Figure S2. Mapping of the affinity versus biophysical properties.

Graphs display the IC_{50} values of gambierol sensitivity for WT and chimeric channels against either the voltage dependence of channel activation in panel **a** or the slope factor in panel **b**. Both analysis clearly indicated that there is no correlation between both parameters, which suggests that the affinity of the chimeres is not determined by their biophysical properties.

Figure S3

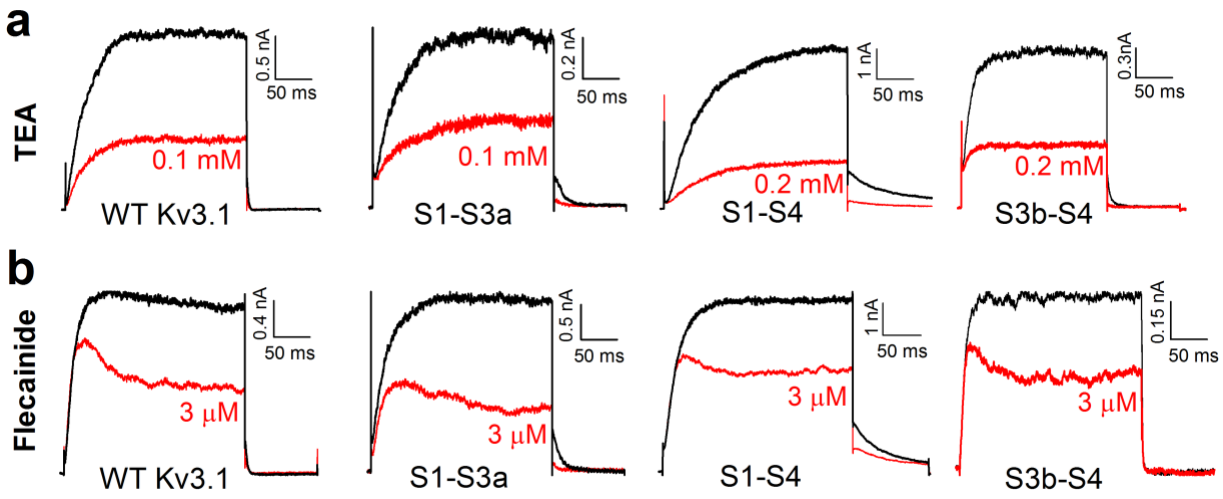

Figure S3. Sensitivity of the different chimeric channels to inhibitors interacting with the pore domain.

a) Current tracings showing the ionic current during a depolarization pulse (WT Kv3.1: +30 mV, S1-S3a: +60 mV, S1-S4: +70 mV, S3b-S4 paddle: + 70 mV) in control (black) and after steady-state inhibition by the external pore blocker TEA (red). **b**) The internal cavity blocker flecainide was tested at depolarization pulses ($V_{1/2}$ + 30 mV) where most of the channels are open. No changes in affinity where observed compared to WT Kv3.1.

Figure S4

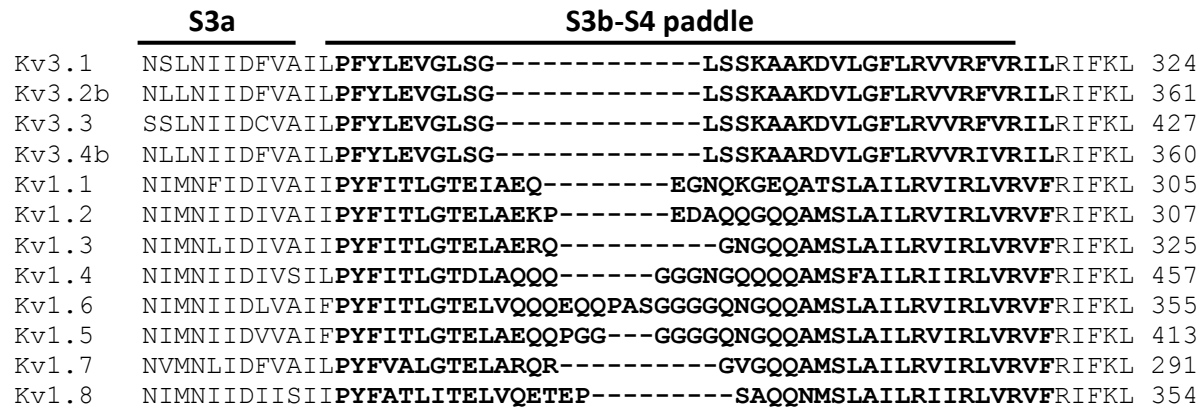

Figure S4. Primary sequence alignment of the S3b-S4 paddle region within Kv3 and Kv1 subfamilies. Whereas the sequence is conserved between Kv3 family members, it is highly variable both in sequence and length between within the Kv1 family.